Talanta 122 (2014) 172–179

Contents lists available at ScienceDirect

Talanta

journal homepage: www.elsevier.com/locate/talanta

# Lipophilicity indices derived from the liquid chromatographic behavior observed under bimodal retention conditions (reversed phase/hydrophilic interaction): Application to a representative set of pyridinium oximes

Victor Voicu [a], Costel Sârbu [b], Florentin Tache [c], Florina Micăle [c], Ştefan Flavian Rădulescu [d], Koichi Sakurada [e], Hikoto Ohta [e], Andrei Medvedovici [c,*]

[a] University of Medicine and Pharmacy "Carol Davilla", Department of Pharmacology, Toxicology and Clinical Psychopharmacology, #8 Floreasca Street, Bucharest 014461, Romania
[b] Babeş-Bolyai University, Faculty of Chemistry and Chemical Engineering, Department of Chemistry, Arany Janos Street, No 11, Cluj-Napoca 400028, Romania
[c] University of Bucharest, Faculty of Chemistry, Department of Analytical Chemistry, Panduri Avenue, No. 90, Bucharest 050663, Romania
[d] University of Medicine and Pharmacy Carol Davila, Faculty of Pharmacy, Department of Drug Industry and Pharmaceutical Biotechnology, Traian Vuia Street # 6, Bucharest 020956, Romania
[e] National Research Institute of Police Science, 6-3-1, Kashiwanoha, Kashiwa, Chiba 277-0882, Japan

ARTICLE INFO

*Article history:*
Received 25 November 2013
Received in revised form
15 January 2014
Accepted 20 January 2014
Available online 31 January 2014

*Keywords:*
Lipophilicity indices
Bimodal chromatographic retention
Pyridinium oximes

ABSTRACT

The liquid chromatographic behavior observed under bimodal retention conditions (reversed phase and hydrophilic interaction) offers a new basis for the determination of some derived lipophilicity indices. The experiments were carried out on a representative group (30 compounds) of pyridinium oximes, therapeutically tested in acetylcholinesterase reactivation, covering a large range of lipophilic character. The chromatographic behavior was observed on a mixed mode acting stationary phase, resulting from covalent functionalization of high purity spherical silica with long chain alkyl groups terminated by a polar environment created through the vicinal diol substitution at the lasting carbon atoms (Acclaim® Mixed Mode HILIC 1 column). Elution was achieved by combining different proportions of 5 mM ammonium formiate solutions in water and acetonitrile. The derived lipophilicity indices were compared with log *P* values resulting from different computational algorithms. The correlations between experimental and computed data sets are significant. To obtain a better insight on the transition from reversed phase to hydrophilic interaction retention mechanisms, the variation of the thermodynamic parameters determined through the van't Hoff approach was also discussed.

© 2014 Elsevier B.V. All rights reserved.

*Abbreviations:* AChE, acetylcholinesterase; AClogP, log *P* estimation according to the ALOGPS 2.1. software (different computational approaches); ALOGP, log *P* estimation according to the Ghose–Crippen algorithm; ALOGPs, log *P* estimation according to the ALOGPS 2.1. software (different computational approaches); CHI, lipophilicity index obtained in fast gradient elution conditions; d.p., diameter of the packed particles (mm); $\Delta G^0$, standard Gibbs free energy; $\Delta H^0$, standard enthalpy; $\Delta S^0$, standard entropy; *F*, flow rate; $\phi$, volume phase ratio ($V_{S.Ph.}/V_{M.Ph.}$); HILIC, hydrophilic interaction liquid chromatography; Hy, hydrophobicity estimation; HYL, linear extrapolation of the retention factor to 100% acetonitrile as mobile phase; i.d., column's internal diameter (mm); ISOELUT, isoelution composition (% of acetonitrile in the mobile phase corresponding to the minimum retention determined through a binomial regression approach); ISOELUT1, isoelution composition (% of acetonitrile in the mobile phase corresponding to the minimum retention determined through a linear regression approach); ISOELUT2, isoelution composition (% of acetonitrile in the mobile phase corresponding to the minimum retention determined through a power regression approach); *k*, retention factor; $k_{min}$, lipophilicity index corresponding to the minimum retention factor experimentally determined; $K_{o/w}$, distribution coefficient between *n*-octanol and water; KOWWIN, log *P* estimation according to the ALOGPS 2.1. software (different computational approaches); $k_w^{bin}$, extrapolated retention factor to 100% aqueous mobile phase through a binomial approach; $k_w^{lin}$, extrapolated retention factor to 100% aqueous mobile phase through a linear approach; *L*, column length (cm); LC–MS, liquid chromatography coupled to mass spectrometric detection; log, mathematical symbol of the logarithm function; log *D*, logarithm of the distribution ratio between n-octanol and water brought to a given pH value; log $k_w$, lipophilicity index resulting from extrapolation of the retention factor to 100% aqueous mobile phase; log *P*, logarithm of $K_{o/w}$; M. Ph., mobile phase; miLogP, log *P* estimation according to the ALOGPS 2.1. software (different computational approaches); MLOGP, log *P* estimation according to Moriguchi; OP, organophosphorus; PC, principal component; PCA, principal component analysis; QSAR, quantitative structure–activity relationship; QSPR, quantitative structure–properties relationships; *R*, universal gas constant (8.31 J $K^{-1}$ $mol^{-1}$); RPLC, reversed phase liquid chromatography; RSD, relative standard deviation; S.Ph., stationary phase; SlogD, log *D* estimation according to ADMET Predictor software, version 5.0.0012; SlogP, log *P* estimation according to ADMET Predictor software, version 5.0.0012; *T*, temperature (°C or K); $t_0$, column's void time; TOC, total residual organic carbon content (ng $mL^{-1}$); XLOGP2, log *P* estimation according to the ALOGPS 2.1. software (different computational approaches); XLOGP3, log *P* estimation according to the ALOGPS 2.1. software (different computational approaches)

* Corresponding author.
*E-mail address:* avmedved@yahoo.com (A. Medvedovici).

0039-9140/$ - see front matter © 2014 Elsevier B.V. All rights reserved.
http://dx.doi.org/10.1016/j.talanta.2014.01.048

## 1. Introduction

Lipophilicity, accepted as an extension of the hydrophobic character, includes all favorable interactions that contribute to the distribution of a chemical entity between water and other solubilizing media, and represents a manifestation of the characteristics of the system in which the solute is placed [1].

The octanol–water distribution coefficient ($K_{o/w}$) got widely acceptance as the physicochemical property measuring the lipophilicity of chemicals [2]. It stands at the basis of quantitative structure–properties/activity relationships (QSPR/QSAR), having crucial roles in various domains, such as fundamental, industrial and food chemistry, pharmaceutical sciences (drug design, prediction of absorption/metabolization/distribution/excretion/toxicological features), environmental risk assessment (bioaccumulation in aquatic biota) and agriculture (soil sorption).

Experimental determination of $K_{o/w}$ is possible through the use of different direct or indirect approaches. Both alternatives were extensively reviewed in the literature [1,3–5]. As the separation methods (and more specifically, the chromatographic ones) are based on distribution of solutes between non-miscible phases, their use in estimation of $K_{o/w}$ is frequent.

No general consensus exists about the ability of reversed phase (RP) chromatography driven on chemically bonded stationary phases to estimate $K_{o/w}$ of chemical compounds. Many efforts have been paid to optimize/standardize the experimental conditions [6,7]. Immobilization of n-octanol and biomimetic moieties (artificial membranes, liposomes) as well as different chemistries of the modification of the silicagel surface was especially tailored to obtain the closest estimation [8–10]. Retention behavior in micellar and microemulsion electrokinetic chromatographic approaches was found highly correlated with $K_{o/w}$ [11,12]. The solvation parameter model acts as a tool frequently used for identification and evaluation of the suitability of a chromatographic system to closely estimate $K_{o/w}$ [13,14]. Undoubtedly, high performance liquid chromatography (HPLC) provides a generous platform for identification and measurement of various types of lipophilicity, resulting in numerous classes of indices, more or less correlated to $K_{o/w}$. Lipophilicity scales, based on different theoretical approaches and determined by different procedures, may somehow overcome the difficulties of standardization. The most used lipophilicity index is the retention factor ($k$) [15]. It was completed by log $k_w$ index, representing the functional extrapolation to a hypothetical situation when the mobile phase is 100% water [16]. The introduction of the chromatographic retention index (CHI) by Valkó et al. leaded to an experimental approach based on fast gradient elution [17]. Sârbu et al. proposed an alternative scale, based on the modification of $k$ on replicate increasing injection volumes of samples obtained in diluents non-miscible with the mobile phase [18]. The image may be completed by the scores obtained through application of the Principal Component Analysis (PCA) to the matrix of the specific retention factors obtained under different elution conditions [19,20]. Based on the previous mentioned approaches, many applications have been published in literature with respect to various classes of compounds, i.e. drugs, natural products, products for food industry, pesticides.

Oxime type reactivators are used as cleavage reagents of the bond between a former serine hydroxyl group situated on the esteratic active site of acetylcholinesterase (AChE) and the phosphorus atom of an inhibitor ((thio)phosphonyl/phosphoryl moiety belonging to a nerve agent or pesticide) [21]. The oximate anion acts as a nucleophilic agent while the quaternary nitrogen favorably positions the reactivator towards an anionic center representing a secondary binding site at the entrance of a narrow gorge of the enzyme. The reactivating potency of an oxime depends on the inhibitory characteristics of the organophosphorus compound (OP), the inter-correlation between spontaneous reactivation and aging processes, as well as on its ability of penetration through biological barriers (mainly the brain–blood one). The existence of quaternary pyridinium nitrogen atoms in the structures of most oximes used as AChE reactivators makes their ability to penetrate through biological barriers difficult [22]. A lot of effort has been made to control the hydrophilic character of a pyridinium oxime through the nature of the substituent of the quaternary nitrogen atom [23]. Thus, it appears important to find practical and fast experimental approaches for establishing the relative change in the hydrophilic character of newly synthesized pyridinium oximes according to the substitution of the quaternary nitrogen atoms. Retention behavior of quaternary oximes on various stationary phases (involving different retention mechanisms), as lipophilicity descriptors, has been discussed in recent publications [24–26].

The aim of the present approach is to evaluate the possibility of measuring lipophilicity indices from the chromatographic behavior obtained under bimodal retention conditions (reversed phase and hydrophilic interaction) on a dodecyl diol chemically modified silicagel as a stationary phase for a set 30 congeners belonging to the mono-pyridinium oxime class. As the retention profiles are “U” shaped, interest was focused on the correlation between the minimum retention conditions and the lipophilic characteristics of the investigated compounds. The experimental values were correlated with log $P$ values deriving from different computational algorithms. Some thermodynamic aspects related to transition from RP to HILIC elution modes are also discussed.

## 2. Experimental

### 2.1. Reagents

Acetonitrile (HPLC gradient grade), and ammonium formate (eluent additive for LC–MS grade) from Merck (Darmstadt, Germany) were used during experiments. Water for chromatography (resistivity of minimum 18.2 MΩ and total residual organic carbon content—TOC—of maximum 30 ng $mL^{-1}$) was produced within the laboratory by means of a TKA Lab HP 6UV/UF instrument (TKA Instruments as part of Thermo Fischer Scientific, Niederelbert, Germany). The chemical structures of the studied analytes are presented in Fig. 1. All compounds were bromide salts, exception being made by PAE-iodide (all position isomers). The studied oximes were synthesized at the National Research Institute of Police Science, Chiba, Japan. The analytes considered in the present approach were specifically selected for an illustrative structure–lipophilicity relationship study and not necessarily for their therapeutic reactivation capacity.

### 2.2. Equipments

Experiments were performed with an Agilent 1260 Infinity series LC/MWD (Agilent Technologies) system consisting of the following modules: quaternary pump (G1311B), automated injector (ALS-G1329B), column thermostat (TCC-G1316C), and a multichannel UV–vis detector (DVL-G1365D). System control and data acquisition were made with the Agilent Chemstation for LC 3D, version 04.03(16).

### 2.3. Chromatographic experiments

An Acclaim™ Mixed-Mode HILIC-1 column (150 mm L × 4.6 mm i.d. × 5 μm d.p.) from Thermo Scientific (P.N. 066843, S.N. 001261) was used and thermostated at 25 °C. The stationary phase consists in a high purity, 120 Å pore size, spherical silicagel

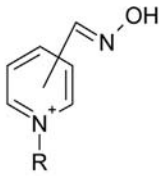


| # | Substituent (R) Name | Substituent (R) Formula | Position of the oxime moiety | Acronym(s) |
|---|---|---|---|---|
| 1 | Ethyl | $-C_2H_5$ | 2, 3, 4 | 2-PAE, 3-PAE, 4-PAE |
| 2 | Butyl | $-C_4H_9$ | 2, 3 | 2-PAB, 3-PAB |
| 3 | Hexyl | $-C_6H_{13}$ | 2, 3, 4 | 2-PAH, 3-PAH, 4-PAH |
| 4 | Octyl | $-C_8H_{17}$ | 2, 3, 4 | 2-PAO, 3-PAO, 4-PAO |
| 5 | Decyl | $-C_{10}H_{21}$ | 2, 3 | 2-PAD, 3-PAD |
| 6 | Dodecyl (Lauryl) | $-C_{12}H_{25}$ | 2, 3, 4 | 2-PAL, 3-PAL, 4-PAL |
| 7 | Benzyl | $-CH_2-C_6H_5$ | 2, 3, 4 | 2-PABn, 3-PABn, 4-PABn |
| 8 | Ethyl-phenyl | $-(CH_2)_2-C_6H_5$ | 2, 3, 4 | 2-PAPE, 3-PAPE, 4-PAPE |
| 9 | Propyl-phenyl | $-(CH_2)_3-C_6H_5$ | 3 | 3-PAPP |
| 10 | Butyl-phenyl | $-(CH_2)_4-C_6H_5$ | 3, 4 | 3-PAPB, 4-PAPB |
| 11 | 4-Methylbenzyl | $-CH_2-C_6H_4-CH_3$ | 2, 3, 4 | 2-PAMB, 3-PAMB, 4-PAMB |
| 12 | 4-*t*-Butylbenzyl | $-CH_2-C_6H_4-C(CH_3)_3$ | 3, 4 | 3-PATB, 4-PATB |

**Fig. 1.** Chemical structures of the compounds considered during the study.

particles chemically functionalized with long chain alkyl groups (dodecyl) terminated by a polar environment created through the vicinal diol substitution at the lasting carbon atoms. Injection volume was 2 μL. Compounds were dissolved in acetonitrile, at a nominal concentration of 1 mg $mL^{-1}$. The components of the mobile phase were 5 mM of ammonium formate in both water (solvent A) and acetonitrile (solvent B). A flow rate of 1 mL $min^{-1}$ was used. Retention profiles of the target analytes were obtained under different isocratic elution conditions, when increasing solvent B proportion from 5% to 90%, in steps of 2.5%, 5% or 10%. The precise conditions used for each analyte are given in the Supplementary material, Part 1, together with the corresponding experimental retention factors. When shifting from a mobile phase composition to another, a minimum 2 h equilibration period was applied. The void time ($t_0$) in the chromatograms was determined through observation of the injection signal. Three replicates were made for each injection. The relative standard deviation (RSD) calculated for the absolute retention times values between triplicates were below 2.0%. Mean absolute retention time values were used for calculation of the retention factor ($k$). Detection was made at 220, 254 and 300 nm ( ± 4 nm), with a reference wavelength of 480 nm ( ± 10 nm).

The study of the thermodynamic aspects occurring during the bimodal separation of oximes on the Acclaim™ Mixed-Mode HILIC-1 column was performed only for 3-PAB. The elution profiles were obtained for 10%, 40%, 55%, 80% and 90% solvent B in the mobile phase, and at 20, 25, 30, 35, 40 and 45 °C (293.15; 298.15; 303.15; 308.15; 313.15; 318.15 K). The van't Hoff functional dependency ln $k=f(1/T)$ was used for the determination of the thermodynamic parameters of standard enthalpy, entropy and free Gibbs energy.

### 2.4. Software

For the investigated analytes, the hydrophobicity index (Hy), the log *P* value calculated according to Moriguchi's method (MLOGP) and the Ghose–Crippen log *P* (ALOGP) were computed by means of the Dragon Plus 5.4 software (www.talete.mi.it). ALOGPS 2.1 software (www.vcclab.org) allowed computation of ALOGPs, AClogP, miLogP, KOWWIN, XLOGP2 and XLOGP3 through different algorithms based on structural, atomistic, topological and electro-topological considerations. log *D* values for the interval of pH from 0 to 14 (1 unit step) were computed with the Marvin Sketch 5.5.01 (www.intro.bio.umb.edu). SlogP and SlogD were calculated through using the ADMET Predictor, vers. 5.0.0012, Simulation Plus Inc. (U.S.A). Some solubilities such as FaSSGF – solubility in fasted state simulated gastric fluid, FaSSIF – solubility in fasted state simulated intestinal fluid, FeSSIF – solubility in fed state simulated intestinal fluid, $P_{eff}$ – human jejunal effective permeability, Diff. coeff. – molecular diffusion coefficient in water, MDCK – apparent MDCK COS permeability, $P_{cornea}$ – permeability through rabbit cornea were also determined by the ADMET Predictor. The logarithm of the brain/blood barrier (log BBB), the percent unbound to blood plasma proteins (PrUnbnd) and the pharmacokinetic volume of distribution in humans ($V_d$) were predicted with the on-line PreADMET software.

Log *P* values computed for the considered compounds are enlisted in Supplementary material, Part 2. One can observe that the computational results are well correlated in-between (correlations coefficients are generally higher than 0.9). Exception is made only by the Hy values, which are less and inversely correlated with the other log *P* data. Supplementary material, Part 3 enlists the values computed for different solubilities and molecular properties (molecular weight and volume, Diff. coeff.). As log *P* may be more or less involved in the computational algorithms of the solubilities, their reciprocal correlations are also mentioned in Part 3. Values calculated for $P_{eff}$, $P_{cornea}$, and PrUnbnd poorly correlate to log *P*.

Log *D* values calculated for all compounds do not significantly vary with the pH in the interval from 3 to 10. This characteristic is well illustrated in Supplementary material, Part 4.

Principal Component Analysis (PCA) computations were performed using Statistica 8.0 software.

## 3. Results and discussions

### 3.1. General considerations

Separation of pyridinium oximes on the alkyl-diol stationary phase is illustrated in Supplementary material, Part 5. Examples cover all available substituents for the quaternary nitrogen atom from the pyridinium ring, and the oxime group is placed in position *meta* (3). Isocratic elution conditions are addressed in the figure and correspond to the minimum retention. Peak symmetry may be considered as acceptable. No peak distortion effects were observable.

Primary data processing consists in calculation of the retention factors $k=(t_R-t_0)/t_0$ of the chromatographic peaks. Two types of plots were primarily used: $k=f(\varphi)$ and log $k=f(\varphi)$, were $\varphi$ is the percentage of the organic solvent in the mobile phase. Examples of the functional dependences are given in Fig. 2, for PAE and PATB analytes, respectively. Retention profiles are always U shaped plots. We focused on the minimum of the retention ($k_{min}$ or log $k_{min}$) and on the composition of the mobile phase enabling the minimal retention ($\varphi$ corresponding to $k_{min}$ or log $k_{min}$), which has been arbitrarily named "isoelution composition" or simply *ISOELUT*. Further on, the names of the hydrophobicity indices derived from the log $k=f(\varphi)$ plots are indicated by the prefix *LOG*.

The left side of the functional dependency profile may be attributed to the RP retention mechanism (retention decreases with the increase of the organic component in the mobile phase) determined by the partition of the analyte between the polar mobile phase and the hydrophobic layer formed by the alkyl moieties chemically bonded to the silicagel surface. The right side of the plot illustrates the HILIC behavior (retention increases with the increase of the organic component). This behavior is determined by the partition of the analyte between the less polar mobile phase and an aqueous layer formed by means of the hydrogen bonds appearing between the diol moiety (positioned at the end of the alkyl chains) and water molecules.

In the case of the minimum retention (bottom of the U shaped retention profile), most probably that both retention mechanisms

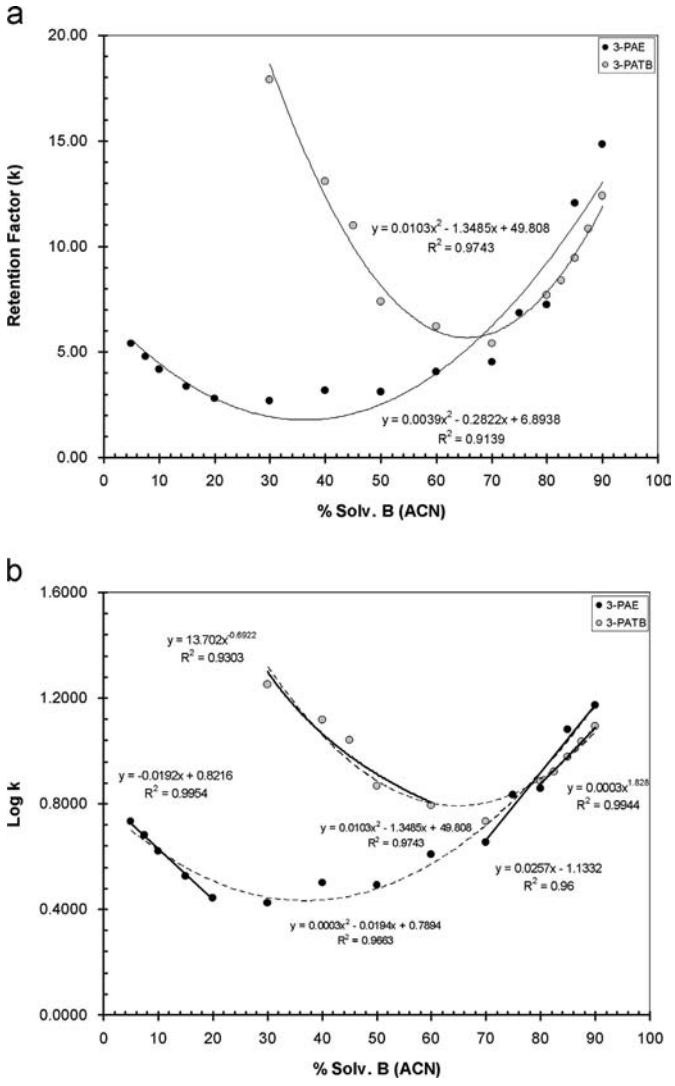


**Fig. 2.** Typical retention profiles of two studied compounds, presented as functional relationships between the content of the organic solvent in the mobile phase ($\varphi$) and the retention factor ($k$) or logarithm of the retention factor ($\log k$), respectively (a and b). Illustration of the different approaches used for determination of the composition of the mobile phase corresponding to the minimum retention (arbitrarily called isoelution composition and denoted as *ISOELUT* or *LOG ISOELUT*).

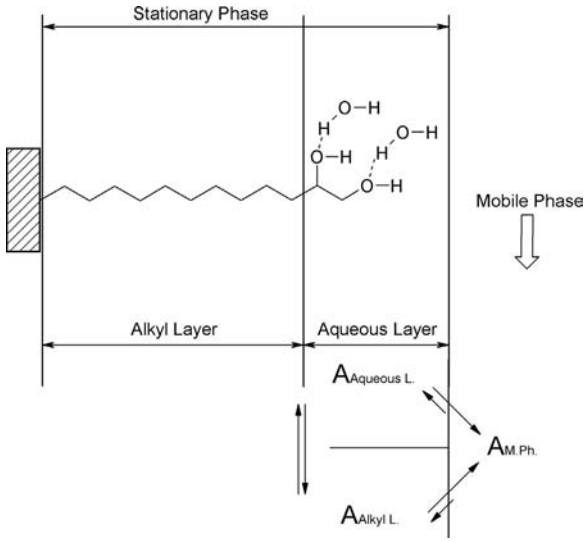


**Fig. 3.** Presumed processes arising at the isoelution interval, as an overlap between reversed phase and hydrophilic interaction mechanisms.

(RP and HI) coexists. As illustrated in Fig. 3, it seems probable that a bilayer is formed on the surface of the silicagel, consisting in the bulk of the alkyl moieties (as hydrophobic media) and the bulk of water molecules retained via hydrogen bonding by the hydroxyl moieties positioned at the extremity of the alkyl chains. The partition of the analyte versus the mobile phase is favored according to both retention models, but elution does not arise at the void time of the column. This means that retention of the analyte is decided by the time spent for the reciprocal transfer within the bilayer generated on the silica surface. Accordingly, the retention factor may be written as $k=K'(V_{alkyl}/V_{aqueous})$, where $V_{alkyl}$ and $V_{aqueous}$ are the volumes of the hydrocarbonaceous/water bulks forming the bilayer, and $K'$ is the distribution constant of the analyte between the alkyl/aqueous layers. If so, the minimum chromatographic retention (expressed as retention factor) should account for the distribution of the analyte between the hydrophobic alkyl layer and the water formed layer, which, at least in theory, should mimic the $K_{o/w}$. Simultaneously, the mobile phase composition granting the minimum retention at the reciprocal compensation between the RP and HI mechanisms should also act as a hydrophobicity index scale.

### 3.2. Hydrophobicity scales

The minimum retention factor ($k_{min}$) and the corresponding logarithm ($\log k_{min}$) can be easily determined from the experimental set of data for each analyte.

The U shaped retention profiles, however, are frequently not symmetrical and vary with respect to their width. The determination of *ISOELUT* or either *LOG ISOELUT* may be achieved in different ways. The simplest approach is to apply a binomial fitting to all experimental values. Once $k$ or $\log k$ are functionally correlated with $\varphi$ through a binomial relationship ($a\varphi^2+b\varphi+c$), the minimum can be easily determined as $-b/2a$.

An alternative approach was to consider only the experimental data obtained on the two sides of the U shaped profile. If a linear fitting model ($b\varphi+a$) is applied to the two sets of data (one for the decreasing side and the other on the increasing one), thus the isoelution composition (noted now *ISOELUT1* or *LOG ISOELUT1*) can be determined through equalization of the linear regressions, by means of the relationship $(a_2-a_1)/(b_1-b_2)$, where $b_1$, $a_1$ and $b_2$, $a_2$ are the slopes and the intercepts of the equations in the RP and HI intervals, respectively. Experimentally, at least five data points were considered for the linear fitting on each side of the U shaped profile. Correlations coefficients describing the linear relationships are given in Supplementary material, Part 6.

Experimental data points on the two sides of the U shaped profiles may be also successfully correlated by means of binomial ($a\varphi^2+b\varphi+c$) or power ($a\varphi^b$) models. Equalizing the binomial equations from the RP and HI sides leads in some cases to imaginary solutions. This was the reason why this alternative has been rejected. Equalizing the power equations and calculation of *ISOELUT*/*LOG ISOELUT* values can be easily done through the relationship $(a_2/a_1)^{\wedge}(1/(b_1-b_2))$, indexes 1 and 2 referring to the RP and HI sides, respectively. The computed values are addressed as *ISOELUT2* and *LOG ISOELUT2*. Correlations coefficients describing the power type relationships are illustrated in the same table, under Supplementary material, Part 6. The minimum number of data points considered for the power regression model on each side of the plots was also 5.

In order to make a comparison to hydrophobicity scales already in use, the values of the retention factor extrapolated to a

hypothetical mobile phase containing 100% water have been computed ($k_w$ and $\log k_w$, respectively). Extrapolation to $\varphi=0$ was made either through linear or binomial fitting models, on the data points determined in the RP zone. These hydrophobicity indices are further noted as $k_w^{lin}$, $\log k_w^{lin}$, $k_w^{bin}$, $\log k_w^{bin}$.

As in Ref. [24] a hydrophilicity scale was proposed through extrapolation to $\varphi=100\%$ on the HI governed side of the retention profiles, calculations were performed based on the linear fitting corresponding equations. These indices, which are theoretically reversely correlated to $\log P$, are further denoted *HYL* or *LOG HYL*.

The values of the hydrophobicity indices derived from the retention profiles of the studied compounds on the Acclaim™ Mixed-Mode HILIC-1 column are enlisted in Table 1. The correlation coefficients established between these indices and the computed $\log P$ values are also presented in Table 1.

One can observe that $k_{min}$, $\log k_{min}$, *ISOELUT* and *LOG ISOELUT* correlate better to all computed $\log P$ values compared to the other determined indices. Indices resulting from consideration of the RP behavior and extrapolation to $\varphi=0\%$ ($k_w^{lin}$, $\log k_w^{lin}$, $k_w^{bin}$, and $\log k_w^{bin}$) are significantly less correlated to computed $\log P$ values, compared to the newly proposed descriptors. Indices resulting from consideration of the HI behavior and extrapolation to $\varphi=100\%$ (*HYL* and *LOG HYL*) have practically no correlation to computed $\log P$ values (correlation coefficients lower than 0.5). The different methodologies used for determination of *ISOELUT*/*LOG ISOELUT* values through separate consideration of the two sides of the U shaped retention profiles (*ISOELUT1*, *ISOELUT2*, *LOG ISOELUT1*, *LOG ISOELUT2*) failed to provide useful results, as long as the correlations with $\log P$ values are significantly lower compared to those resulting from the consideration of the entire retention profile. It seems that the binomial regression model applied to the experimental data points induces less error, despite the asymmetry of the U shaped profiles, in evaluating of the mobile phase composition corresponding to the minimum of retention. If making a comparison between the newly determined indices, $k_{min}$ and $\log k_{min}$ performed better compared to *ISOELUT* and *LOG ISOELUT*. A graphic illustration of the correlation established between the determined $\log k_{min}$ and the XLOGP3 computed values is given in Fig. 4.

As already highlighted in [27], $\log P$ values resulting from different computational models are more or less correlated to other molecular descriptors (i.e. molecular weight, molecular volume), BCS-correlated parameters (i.e. solubilities in simulated biological fluids, permeabilities across biological membranes) and quantitative predictions of penetration across biological barriers (i.e. blood brain barrier, Caco II cells). The newly proposed hydrophobicity indices, namely $k_{min}$, $\log k_{min}$, *ISOELUT* and *LOG ISOELUT*, were assessed for their correlations with some of the parameters computed via the PreADMET and ADMET Predictor softwares. Results are presented in Table 2.

For simple comparison purposes, correlations of the determined $k_w^{lin}$ and $\log k_w^{lin}$ were added to Table 2. One can observe that the new indices are fairly correlated with most of the parameters taken into consideration, and in some cases are superior to correlations between these parameters and the computed $\log P$ values (if compared to data from Supplementary material, Part 3). Additionally, the proposed indices perform better than those based on extrapolation of retention to $\varphi=0\%$ under RP conditions.

### 3.3. PCA approach

As mentioned above, during the last decade, new insights were offered by PCA which has the ability to provide highly descriptive lipophilicity indices. PCA is extracting the meaningful and interpretable features from the underlying information of the multivariate raw data. It has the ability to separate the pertinent information from the noise. Usually, the first few components account for the maximum information existing in the initial (raw) data. Basically in our particular case the lipophilicity descriptor is the score corresponding to the first principal components (*PC1*), obtained by applying the PCA algorithm on the covariance matrix formed by the $k$ and $\log k$ values of the target compounds obtained for each mobile phase level. Moreover, the representation of the scores corresponding to the first two principal components may offer a suggestive clustering of investigated compounds giving new insights concerning their (dis) similarity and possible outliers.

Even if the correlations between the scores corresponding to the first principal component obtained by applying PCA to the covariance matrix of $k$ and $\log k$ values and the computed descriptors are not highly significant (Supplementary material, Part 7), the pattern obtained by plotting the scores corresponding to the first two principal components is highly informative. However, as it is illustrated in Fig. 5 for $\log k$ data, the scores plot is very useful as a display tool for examining the relationships between compounds, looking for trends, groupings or outliers. It appears clearly that the compounds studied in this work form two well defined clusters, a linear cluster (*n*-alkyl substituents of the pyridinium nitrogen atom) and a more heterogeneous cluster (aromatic substitution of the nitrogen atom) in a good agreement with their chemical structure.

The loadings representation obtained by applying the PCA algorithm on the matrices (30 rows and 27 or 16 columns) formed by lipophilicity descriptors computed using different algorithms and/or the indices estimated from experimental data may offer suggestive (dis)similarity charts. By a careful examination of this kind of patterns (see Fig. 6), it is easy to observe three distinct clusters and the outlier position of Hy. The first cluster includes only $\log k_w^{bin}$ and *PC*1/$\log k$, the second one is formed by all $\log P$/$\log D$ computed descriptors and the following experimental lipophilicity indices: $k_{min}$, $\log k_{min}$, *ISOELUT*, *LOG ISOELUT*, $k_w^{lin}$, $\log k_w^{lin}$, $k_w^{bin}$, $\log k_w^{bin}$, and *PC*1/$\log k$. The third cluster contains the following experimental lipophilicity indices: *ISOELUT 1*, *LOGISOELUT 1*, *ISOELUT 2*, *LOG ISOELUT 2*, *HYL*, *LOG HYL*, and *PC*1/$k$.

A similar pattern results after examination of the loadings of the PCA algorithm applied only on the set of experimentally determined indices (see Supplementary material, Part 8).

### 3.4. Thermodynamic considerations

To obtain a better insight on the thermodynamic processes appearing on transition from RP to HI retention mechanisms, the standard enthalpy ($\Delta H^0$), the entropic contribution ($\Delta S^0/R+$ volume phase ratio) and the standard Gibbs free energy ($\Delta G^0$) were estimated for 3-PAB, at different mobile phase compositions ($\varphi=10\%$, 40%, 55%, 80% and 90%).

The transfer of the analyte from the mobile phase (M.Ph.) to the stationary phase (S.Ph) is thermodynamically characterized by $\Delta G^0$ ($\Delta G^0=\Delta H^0-T\Delta S^0$). $\Delta H^0$ and $\Delta S^0$ are readily available experimentally from the retention study of the analyte in isocratic elution conditions for a specified mobile phase composition and different temperatures (20, 25, 30, 35, 40, and 45 °C were chosen in our study), through the vant'Hoff equation, namely $\ln k=B/T+A=-\Delta H^0/R/T+(\Delta S^0/R+\ln\phi)$. In the former relationships, $R$ is the universal gas constant (8.31 J K$^{-1}$ mol$^{-1}$) and $\phi$ is the volume phase ratio ($V_{S.Ph.}/V_{M.Ph.}$).

The functional dependencies $\ln k=f(1/T)$ for 3-PAB were found linear in the studied temperature interval and mobile phase compositions, as one can observe from values enlisted in Table 3. The experimental retention data used to generate information in Table 3 may be found in the Supplementary material, Part 9.

**Table 1**
Hydrophobicity indices derived from the retention behavior of studied pyridinium oximes under bimodal retention conditions and their correlations to log *P*/log *D* values computed through different algorithms.

| # | Compound | $k_{min}$ | log $k_{min}$ | ISOELUT | LOG ISOELUT | ISOELUT 1 | LOG ISOELUT 1 | ISOELUT 2 | LOG ISOELUT2 | $k_w^{lin}$ | log $k_w^{lin}$ | $k_w^{bin}$ | log $k_w^{bin}$ | HYL | LOG HYL |
|---|---|---|---|---|---|---|---|---|---|---|---|---|---|---|---|
| 1 | 2-PAE | 2.82 | 0.45 | 37.22 | 33.33 | 52.96 | 42.19 | 56.56 | 51.04 | 6.97 | 0.88 | 8.85 | 1.00 | 18.75 | 1.41 |
| 2 | 3-PAE | 2.66 | 0.43 | 36.18 | 32.33 | 55.63 | 43.53 | 56.77 | 52.31 | 6.08 | 0.82 | 6.91 | 0.86 | 19.45 | 1.43 |
| 3 | 4-PAE | 2.81 | 0.45 | 37.47 | 34.00 | 54.76 | 44.29 | 58.11 | 96.98 | 6.82 | 0.88 | 7.87 | 0.92 | 18.79 | 1.41 |
| 4 | 2-PAB | 4.01 | 0.60 | 48.15 | 48.83 | 38.18 | 40.35 | 57.80 | 69.46 | 18.26 | 1.35 | 24.57 | 1.48 | 16.26 | 1.32 |
| 5 | 3-PAB | 3.71 | 0.57 | 46.62 | 45.33 | 41.53 | 41.53 | 58.53 | 59.18 | 14.29 | 1.23 | 19.07 | 1.36 | 15.65 | 1.31 |
| 6 | 2-PAH | 5.59 | 0.75 | 58.51 | 62.33 | 40.84 | 49.67 | 62.41 | 66.78 | 38.97 | 1.74 | 52.10 | 1.76 | 15.05 | 1.24 |
| 7 | 3-PAH | 4.80 | 0.68 | 56.52 | 58.33 | 44.79 | 52.76 | 66.18 | 72.87 | 29.22 | 1.59 | 41.91 | 1.73 | 15.40 | 1.28 |
| 8 | 4-PAH | 5.17 | 0.71 | 57.58 | 59.17 | 41.58 | 49.51 | 66.93 | 66.81 | 32.83 | 1.65 | 47.94 | 1.81 | 14.44 | 1.23 |
| 9 | 2-PAO | 6.03 | 0.78 | 61.56 | 58.38 | 64.91 | 66.77 | 72.79 | 74.72 | 82.13 | 2.52 | 75.97 | 1.18 | 48.67 | 1.86 |
| 10 | 3-PAO | 5.64 | 0.75 | 60.83 | 60.71 | 66.43 | 66.81 | 71.86 | 69.95 | 64.44 | 2.36 | 126.84 | 2.50 | 44.69 | 1.82 |
| 11 | 4-PAO | 5.57 | 0.75 | 61.32 | 64.43 | 65.19 | 66.83 | 72.81 | 69.19 | 71.76 | 2.43 | 102.47 | 1.62 | 44.34 | 1.82 |
| 12 | 2-PAD | 7.46 | 0.87 | 66.18 | 66.89 | 69.76 | 67.48 | 69.47 | 69.15 | 86.07 | 3.06 | 77.91 | 0.11 | 45.89 | 1.80 |
| 13 | 3-PAD | 6.90 | 0.84 | 66.43 | 70.75 | 70.03 | 68.87 | 72.07 | 70.55 | 73.71 | 2.77 | 61.19 | 0.99 | 40.03 | 1.74 |
| 14 | 2-PAL | 9.66 | 0.98 | 70.50 | 69.35 | 78.03 | 76.69 | 78.13 | 78.75 | 57.35 | 2.34 | 82.94 | 1.58 | 45.59 | 1.76 |
| 15 | 3-PAL | 8.85 | 0.95 | 69.86 | 70.40 | 77.88 | 76.23 | 77.08 | 77.10 | 50.38 | 2.27 | 91.93 | 2.22 | 44.17 | 1.76 |
| 16 | 4-PAL | 8.70 | 0.94 | 70.21 | 70.80 | 78.16 | 76.77 | 78.37 | 75.96 | 50.88 | 2.27 | 80.39 | 1.70 | 43.49 | 1.76 |
| 17 | 2-PABn | 4.25 | 0.63 | 46.25 | 49.63 | 80.00 | 72.83 | 79.56 | 80.03 | 15.88 | 1.26 | 20.96 | 1.40 | 55.31 | 1.95 |
| 18 | 3-PABn | 4.06 | 0.61 | 45.25 | 47.38 | 79.36 | 70.01 | 78.56 | 74.61 | 14.16 | 1.23 | 17.51 | 1.26 | 51.34 | 1.91 |
| 19 | 4-PABn | 4.15 | 0.62 | 45.95 | 47.88 | 78.89 | 70.07 | 77.88 | 80.16 | 14.93 | 1.26 | 17.83 | 1.26 | 49.29 | 1.88 |
| 20 | 2-PAPE | 4.63 | 0.67 | 55.35 | 59.17 | 54.68 | 57.37 | 70.00 | 70.64 | 24.02 | 1.51 | 27.46 | 1.39 | 18.72 | 1.40 |
| 21 | 3-PAPE | 4.45 | 0.65 | 54.74 | 57.83 | 55.04 | 56.81 | 69.75 | 79.82 | 21.46 | 1.46 | 22.39 | 1.27 | 17.47 | 1.36 |
| 22 | 4-PAPE | 4.48 | 0.65 | 55.77 | 60.67 | 54.39 | 57.66 | 71.67 | 72.88 | 23.76 | 1.51 | 25.80 | 1.34 | 17.67 | 1.37 |
| 23 | 2-PAMB | 4.93 | 0.69 | 57.60 | 52.75 | 54.00 | 58.59 | 67.97 | 68.09 | 26.28 | 1.56 | 40.79 | 1.97 | 16.20 | 1.31 |
| 24 | 3-PAMB | 4.73 | 0.68 | 57.03 | 52.63 | 44.16 | 49.69 | 60.05 | 63.73 | 31.98 | 1.77 | 31.96 | 1.36 | 15.23 | 1.27 |
| 25 | 4-PAMB | 4.71 | 0.67 | 58.14 | 51.38 | 42.61 | 51.90 | 64.95 | 64.47 | 36.26 | 1.73 | 43.47 | 1.62 | 14.85 | 1.26 |
| 26 | 3-PAPP | 4.79 | 0.68 | 54.11 | 50.80 | 79.10 | 72.21 | 77.81 | 75.64 | 22.24 | 1.53 | 26.58 | 1.32 | 41.72 | 1.70 |
| 27 | 3-PAPB | 5.04 | 0.70 | 60.22 | 57.63 | 66.58 | 66.53 | 67.44 | 71.04 | 15.61 | 1.32 | 26.42 | 1.71 | 14.55 | 1.25 |
| 28 | 4-PAPB | 5.04 | 0.70 | 60.65 | 59.13 | 66.07 | 66.21 | 66.89 | 68.82 | 16.43 | 1.35 | 29.41 | 1.83 | 14.34 | 1.24 |
| 29 | 3-PATB | 5.39 | 0.73 | 65.46 | 70.88 | 68.12 | 68.47 | 71.41 | 70.62 | 29.46 | 1.75 | 43.46 | 1.85 | 16.92 | 1.30 |
| 30 | 4-PATB | 5.56 | 0.75 | 67.72 | 65.70 | 62.87 | 66.28 | 69.33 | 70.78 | 42.78 | 2.02 | 71.65 | 2.06 | 14.71 | 1.24 |

**Correlation coefficients**

| Correlated sets | ALOGPs | AC logP | miLogP | KOWWIN | XLOGP2 | XLOGP3 | Hy | MLOGP | ALOGP | log D7 | SlogD7.4 |
|---|---|---|---|---|---|---|---|---|---|---|---|
| $k_{min}$ | **0.958** | **0.977** | **0.934** | **0.963** | **0.977** | **0.983** | −0.758 | **0.935** | **0.943** | ***0.884*** | **0.969** |
| log $k_{min}$ | **0.938** | **0.977** | **0.927** | **0.973** | **0.964** | **0.978** | −***0.849*** | **0.954** | **0.944** | **0.918** | **0.969** |
| ISOELUT | ***0.842*** | **0.915** | ***0.835*** | **0.942** | ***0.895*** | ***0.899*** | −***0.891*** | **0.914** | **0.904** | **0.931** | **0.902** |
| LOG ISOELUT | ***0.809*** | ***0.881*** | ***0.810*** | **0.904** | ***0.865*** | ***0.873*** | −***0.874*** | ***0.880*** | ***0.855*** | ***0.894*** | ***0.864*** |
| ISOELUT 1 | 0.479 | 0.512 | 0.460 | 0.508 | 0.484 | 0.529 | −0.518 | 0.577 | 0.393 | 0.537 | 0.503 |
| LOG ISOELUT 1 | 0.678 | 0.740 | 0.661 | 0.752 | 0.700 | 0.750 | −***0.817*** | ***0.806*** | 0.640 | 0.788 | 0.738 |
| ISOELUT 2 | 0.552 | 0.598 | 0.526 | 0.602 | 0.558 | 0.621 | −0.730 | 0.668 | 0.493 | 0.642 | 0.609 |
| LOG ISOELUT2 | 0.193 | 0.209 | 0.117 | 0.214 | 0.201 | 0.226 | −0.267 | 0.240 | 0.135 | 0.232 | 0.227 |
| $k_w^{lin}$ | 0.788 | 0.784 | 0.767 | 0.753 | 0.793 | 0.787 | −0.546 | ***0.803*** | 0.770 | 0.652 | 0.770 |
| log $k_w^{lin}$ | ***0.847*** | ***0.862*** | ***0.836*** | ***0.843*** | ***0.862*** | ***0.863*** | −0.672 | ***0.878*** | ***0.840*** | 0.766 | ***0.845*** |
| $k_w^{bin}$ | 0.754 | ***0.812*** | 0.756 | 0.787 | ***0.817*** | ***0.800*** | −0.570 | ***0.814*** | 0.778 | 0.714 | 0.771 |
| log $k_w^{bin}$ | 0.139 | 0.278 | 0.202 | 0.304 | 0.246 | 0.239 | −0.377 | 0.257 | 0.259 | 0.374 | 0.230 |
| HYL | 0.488 | 0.472 | 0.479 | 0.413 | 0.458 | 0.502 | −0.327 | 0.520 | 0.363 | 0.363 | 0.464 |
| LOG HYL | 0.430 | 0.405 | 0.420 | 0.346 | 0.400 | 0.440 | −0.245 | 0.464 | 0.298 | 0.291 | 0.396 |

Bold values indicate correlation coefficients above 0.9. Bold and italic values indicates correlation coefficients placed within 0.8–0.9 interval.

From the same Table 3, one can also observe that shifting from the RP mechanism to the HI one, the standard enthalpy continuously increases from −8.75 to −1.51 kJ $K^{-1}$ $mol^{-1}$ and the entropic contribution also increases. One can state that the RP retention mode is enthalpy driven while the HI retention is compensated by entropy. On the U shaped retention profile, two compositions of the mobile phase ensure the same retention under two different mechanisms (RP and HI), and consequently are characterized by the same free Gibbs energy. This situation can be described by the following equations:

$$k_{RP} = k_{HI} \Rightarrow \Delta G^0_{RP} = \Delta G^0_{HI} \Rightarrow \Delta H^0_{RP} - T\Delta S^0_{RP} = \Delta H^0_{HI} - T\Delta S^0_{HI}$$
$$\Rightarrow \Delta H^0_{RP} - \Delta H^0_{HI} = T(\Delta S^0_{RP} - \Delta S^0_{HI})$$

As from the van't Hoff equation $\Delta H^0 = -RB$ and $\Delta S^0 = R(A - \ln V_{S.Ph.}/V_{M.Ph.})$, one can easily determine the following equality:

$$\frac{(B_{HI} - B_{RP}) + T(A_{HI} - A_{RP})}{T} = \left(\ln \frac{V^{HI}_{S.Ph.}}{V_{M.Ph.}} - \ln \frac{V^{RP}_{S.Ph.}}{V_{M.Ph.}}\right) = \ln \frac{V^{HI}_{S.Ph.}}{V^{RP}_{S.Ph.}}$$

Under RP mechanism, S.Ph. should be considered as the bulk alkyl moieties chemically immobilized on the silicagel surface. Under the HI mechanism, S.Ph. should be considered as the aqueous layer retained by means of hydrogen bonding to the terminal α-positioned aliphatic hydroxyl groups

If $V_{M.Ph.}$ is experimentally available from $t_0F$ ($F$ is the flow rate), $V^{RP}_{S.Ph.}$ is from far more difficult to approximate. It should not be considered as the volume of the bulk solid material packed in the column, but the volume of the chemical coverage, the dodecyl diol moieties, respectively, in the particular case of the Acclaim™ Mixed-Mode HILIC-1 column. This data was not available from the column manufacturer, but in a first instance it may be approximated with the volume of an octadecyl stationary phase identical as particle size and packed in a column of identical dimensions (around 0.12 mL). If considering experimental data obtained for the paired situations corresponding to $\varphi = 40\%$ and 55% and

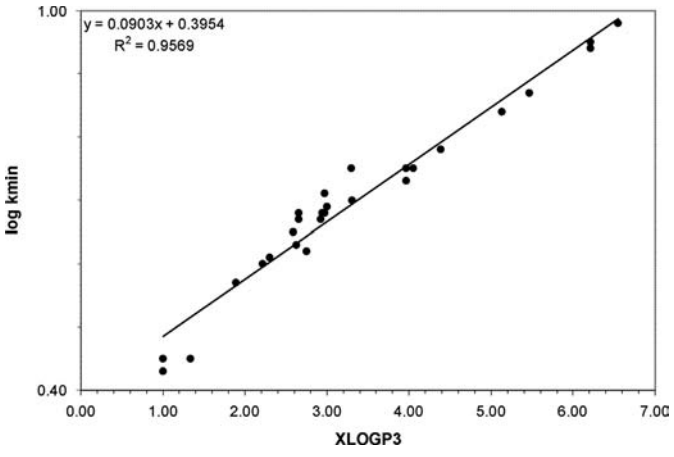


**Fig. 4.** Illustrative graphic correlation between the experimental log $k_{min}$ hydrophobicity descriptor and log $P$ (XLOGP3 computational descriptor).

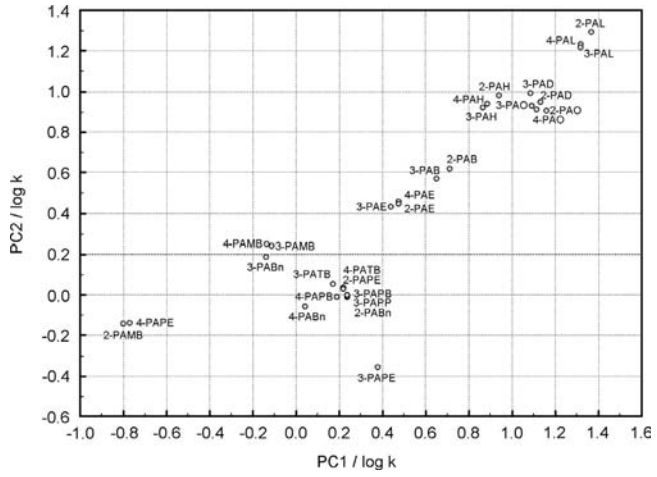


**Fig. 5.** Pattern obtained by plotting the scores corresponding to the first two principal components obtained by applying the PCA algorithm on the covariance matrix formed by the log $k$ values of the target compounds obtained for each mobile phase composition as a display tool designed for examination of (dis) similarities between studied compounds.

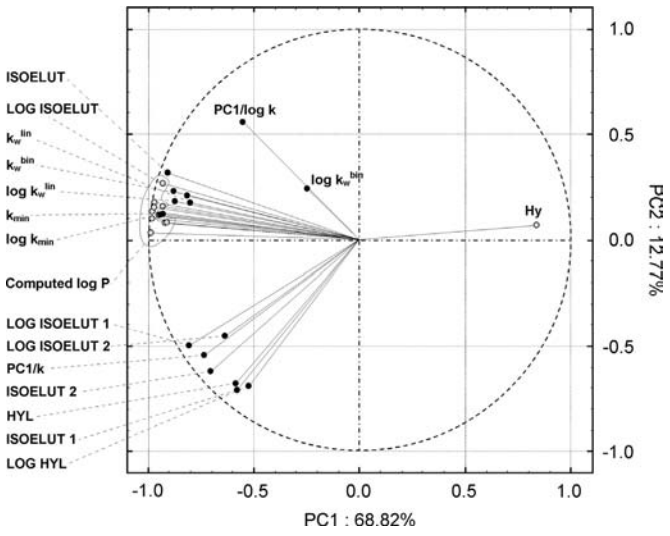


**Fig. 6.** The loadings representation resulting after application of the PCA algorithm on the matrix formed by the computed lipophilicity descriptors and indices estimated from experimental data (values and order according to Table 1).

**Table 2**
Correlations between the indices derived from the behavior of studied compounds under bimodal retention conditions and other molecular descriptors, BCS-correlated parameters and quantitative estimations of penetration across biological barriers/membranes (significance of the acronyms are given in Section 2.4).

| Descriptors | Mw | Mol. vol. | Diff. coef. | $P_{eff}$ | Log (MDCK COS) | $P_{cornea}$ | Log (Sw) | Log (FaSSGF) | Log (FaSSIF) | Log (FeSSIF) | Log BBB | PrUnbnd | Vd |
|---|---|---|---|---|---|---|---|---|---|---|---|---|---|
| $k_{min}$ | 0.861 | 0.946 | −0.887 | 0.711 | −0.764 | 0.304 | −0.899 | −0.969 | −0.859 | −0.894 | 0.852 | −0.416 | 0.889 |
| log $k_{min}$ | 0.909 | 0.967 | −0.953 | 0.726 | −0.728 | 0.401 | −0.939 | −0.966 | −0.924 | −0.932 | 0.792 | −0.539 | 0.884 |
| ISOELUT | 0.929 | 0.950 | −0.971 | 0.776 | −0.707 | 0.512 | −0.941 | −0.923 | −0.931 | −0.949 | 0.648 | −0.629 | 0.849 |
| LOG ISOELUT | 0.894 | 0.914 | −0.947 | 0.729 | −0.633 | 0.486 | −0.900 | −0.884 | −0.905 | −0.905 | 0.647 | −0.622 | 0.836 |
| $k^{lin}_w$ | 0.600 | 0.720 | −0.717 | 0.438 | −0.687 | 0.105 | −0.661 | −0.736 | −0.673 | −0.708 | 0.754 | −0.205 | 0.629 |
| log $k^{lin}_w$ | 0.724 | 0.820 | −0.822 | 0.544 | −0.709 | 0.217 | −0.774 | −0.827 | −0.777 | −0.809 | 0.768 | −0.339 | 0.732 |

**Table 3**
Data resulting from the van't Hoff functional representation ln $k=f(1/T)$ accounting for the thermodynamic aspects of the chromatographic separation based on the bimodal retention mechanism.

| $\varphi$ | $B$ | $A$ | $r_{xy}$ | $\Delta H^0$ (kJ K$^{-1}$ mol$^{-1}$) | $\Delta S^0$ (J K$^{-1}$ mol$^{-1}$) | $\Delta G^0$/25 °C (kJ K$^{-1}$ mol$^{-1}$) |
|---|---|---|---|---|---|---|
| 10 | 1052.5 | −1.611 | 0.9980 | −8.75 | 6.38 | −10.65 |
| 40 | 912.5 | −1.722 | 0.9939 | −7.59 | 4.93 | −9.05 |
| 55 | 858.2 | −1.457 | 0.9958 | −7.14 | 7.13 | −9.26 |
| 80 | 526.7 | 0.004 | 0.9981 | −4.38 | 19.93 | −10.32 |
| 90 | 181.5 | 1.939 | 0.9993 | −1.51 | 35.80 | −12.18 |

$\varphi=10\%$ and 80%, one can conclude that the volume of the aqueous layer is fairly approximating the volume of the bulk alkyl moieties.

## 4. Conclusions

The U shaped retention profiles of a series of alkyl pyridinium mono-oximes obtained on a stationary phase working in bimodal conditions (RP and HI) were determined. It has been demonstrated that the minimum retention ($k_{min}$ or log $k_{min}$) and the isoelution composition (*ISOELUT* or *LOG ISOELUT*) corresponding to the minimum retention can act as powerful index scales well correlated to log $P$ values resulting from different computational algorithms. These hydrophobicity indices were better correlated to log $P$ values than conventional indices resulting from extrapolation of the retention to hypothetical mobile phase compositions of $\varphi=0\%$ or 100%, through linear or binomial models. The isoelution composition corresponding to the minimum retention was determined through three different alternatives: (*a*) the minimum of the binomial equation resulting after the fitting of the experimental data; (*b*) the solution resulting from equalizing the linear fitting equations obtained on the RP and HI sides of the retention profiles; (*c*) the solution resulting from equalizing the power fitting equations obtained on the RP and HI sides of the retention profiles. It has been demonstrated that the simplest approach (alternative *a*) produces indices being more correlated to log $P$ values. The proposed hydrophobicity indices are also fairly correlated to other molecular descriptors (i.e. molecular weight, molecular volume), BCS-correlated parameters (i.e. solubilities in simulated biological fluids, permeabilities across biological membranes) and quantitative predictions of penetration across biological barriers (i.e. blood brain barrier, Caco II cells). The first principal components (*PC1*) resulting from application of the PCA algorithm on the covariance matrix formed by the $k$ and log $k$ values of the target compounds at each mobile phase level are less correlated to log $P$ values compared to the proposed hydrophobicity indices. From the thermodynamic point of view, it has been demonstrated that the RP retention mode is enthalpy driven while the HI retention mode is entropy compensated. This is confirming somehow the hypothesis that at the minimum of the U shaped profile, retention is determined through the partition between a bilayered system represented by the bulk alkyl moieties immobilized to the silicagel surface and an aqueous layer retained by means of hydrogen bonding at the level of the terminating diol moieties. This may explain qualitatively the fair interrelationship between computed log $P$ values and the proposed hydrophobicity indices.

The retention behavior on bimodally (RP and HI) acting stationary phases may be useful in elaboration of hydrophobicity scales based on the proposed indices for various classes of compounds with structural particularities which are rendering difficult the application of conventional approaches resulting from mono-modal chromatographic retention behaviors.

## Acknowledgments

Some of the authors (V.V., Ş.F.R, and A.V.M.) acknowledge the financial support given by the Romanian project PN-II-ID-PCE-2012-4-0651.

## Appendix A. Supporting information

Supplementary data associated with this article can be found in the online version at http://dx.doi.org/10.1016/j.talanta.2014.01.048.

## References

[1] S.K. Poole, S.F. Poole, J. Chromatogr. B 797 (2003) 3–19.
[2] A. Leo, C. Hansch, C. Church, J. Med. Chem. 12 (1969) 766–771.
[3] L.G. Danielsson, Y.H. Zhang, Trends Anal. Chem. 15 (1996) 188–196.
[4] K. Valkó, J. Chromatogr. A 1037 (2004) 299–310.
[5] A. Bethod, S. Carda-Broch, J. Chromatogr. A 1037 (2004) 3–14.
[6] C. Giaginis, S. Theocharis, A. Tsantili-Kakoulidou, Anal. Chim. Acta 573–574 (2006) 311–318.
[7] P.A. Tate, J.G. Dorsey, J. Chromatogr. A 1042 (2004) 37–48.
[8] J. Kotecha, S. Shah, I. Rathod, G. Subbaiah, Int. J. Pharm. 333 (2007) 127–135.
[9] T. Österberg, M. Svensson, P. Lundahl, Eur. J. Pharm. Sci. 12 (2001) 427–439.
[10] F. Barbato, M.I. La Rotonda, F. Quaglia, Eur. J. Med. Chem. 31 (1996) 311–318.
[11] L. Escuder-Gilabert, J.M. Sanchis-Mallols, S. Sagrado, M.J. Medina-Hernández, R.M. Villanueva-Camanas, J. Chromatogr. A 823 (1998) 549–559.
[12] S.K. Poole, D. Durham, C. Kibbey, J. Chromatogr. B 745 (2000) 117–126.
[13] C.F. Poole, S.N. Atapattu, S.K. Poole, A.K. Bell, Anal. Chim. Acta 652 (2009) 32–53.
[14] D. Benhaim, E. Grushka, J. Chromatogr. A 1217 (2010) 65–74.
[15] P. Haber, T. Baczek, R. Kaliszan, L.R. Snyder, J.W. Dolan, C.T. Wehr, J. Chromatogr. Sci. 38 (2000) 386–392.
[16] K. Valkó, V. Slégel, J. Chromatogr. A 631 (1993) 49–61.
[17] C. Bevan, D. Reynolds, Anal. Chem. 69 (1997) 2022–2029.
[18] C. Sârbu, R.D. Naşcu-Briciu, D. Casoni, A. Kot-Wasik, A. Wasik, J. Namiésnik, J. Chromatogr. A 1266 (2012) 53–60.
[19] R.D. Briciu, A. Kot-Wasik, J. Namiésnik, C. Sârbu, J. Sep. Sci. 32 (2009) 2066–2074.
[20] A. Detroyer, V. Schoonjans, F. Questier, Y. Vander Heyden, A.P. Borosy, Q. Guo, D.L. Massart, J. Chromatogr. A 897 (2000) 23–36.
[21] V. Voicu, F.Ş. Rădulescu, A. Medvedovici, Exp. Opin. Drug Metab. Toxicol. 9 (2013) 31–50.
[22] V.A. Voicu, J. Bajgar, A. Medvedovici, F.Ş. Rădulescu, D.S. Miron, J. Appl. Toxicol. 30 (2010) 719–729.
[23] H. Ohta, T. Ohmori, S. Suzuki, H. Ykegaya, K. Sakurada, T. Takatori, Pharm. Res. 23 (2006) 2827–2833.
[24] V. Voicu, I. Sora, C. Sârbu, V. David, A. Medvedovici, J. Pharm. Biomed. Anal. 52 (2010) 508–516.
[25] V. Dohnal, K. Musilek, K. Kuca, J. Chromatogr. Sci. 52 (2014) 246–251.
[26] K. Musilek, J. Jampilek, J. Dohnal, D. Jun, F. Gunn-Moore, M. Dolezal, K. Kuca, Anal. Bioanal. Chem. 391 (2008) 367–372.
[27] F.Ş. Rădulescu, V.A. Voicu, D.S. Miron, C. Mircioiu, C. Drăghici, Rev. Chem. (Buchar.) 62 (2011) 601–605.